

Detecting anatomical characteristics of single motor units by combining high density electromyography and ultrafast ultrasound: a simulation study

*Original*

Detecting anatomical characteristics of single motor units by combining high density electromyography and ultrafast ultrasound: a simulation study / Carbonaro, M.; Zaccardi, S.; Seoni, S.; Meiburger, K. M.; Botter, A.. - ELETTRONICO. - 2022:(2022), pp. 748-751. (Intervento presentato al convegno 44th Annual International Conference of the IEEE Engineering in Medicine and Biology Society, EMBC 2022 tenutosi a Glasgow, Scotland, United Kingdom nel 11-15 July 2022) [10.1109/EMBC48229.2022.9871578].

*Availability:*

This version is available at: 11583/2979695 since: 2023-06-29T12:36:51Z

*Publisher:*

Institute of Electrical and Electronics Engineers Inc.

*Published*

DOI:10.1109/EMBC48229.2022.9871578

*Terms of use:*

This article is made available under terms and conditions as specified in the corresponding bibliographic description in the repository

*Publisher copyright*

IEEE postprint/Author's Accepted Manuscript

©2022 IEEE. Personal use of this material is permitted. Permission from IEEE must be obtained for all other uses, in any current or future media, including reprinting/republishing this material for advertising or promotional purposes, creating new collecting works, for resale or lists, or reuse of any copyrighted component of this work in other works.

(Article begins on next page)

# Detecting anatomical characteristics of single motor units by combining high density electromyography and ultrafast ultrasound: a simulation study

Marco Carbonaro, *Student Member, IEEE*, Silvia Zaccardi, Silvia Seoni, *Student Member, IEEE*  
Kristen M. Meiburger, *Member, IEEE*, and Alberto Botter, *Member, IEEE*

**Abstract**— Muscle force production is the result of a sequence of electromechanical events that translate the neural drive issued to the motor units (MUs) into tensile forces on the tendon. Current technology allows this phenomenon to be investigated non-invasively. Single MU excitation and its mechanical response can be studied through high-density surface electromyography (HDsEMG) and ultrafast ultrasound (US) imaging respectively. In this study, we propose a method to integrate these two techniques to identify anatomical characteristics of single MUs. Specifically, we tested two algorithms, combining the tissue velocity sequence (TVS, obtained from ultrafast US images), and the MU firings (extracted from HDsEMG decomposition). The first is the Spike Triggered Averaging (STA) of the TVS based on the occurrences of individual MU firings, while the second relies on the correlation between the MU firing patterns and the TVS spatio-temporal independent components (STICA). A simulation model of the muscle contraction was adapted to test the algorithms at different degrees of neural excitation (number of active MUs) and MU synchronization. The performances of the two algorithms were quantified through the comparison between the simulated and the estimated characteristics of MU territories (size, location). Results show that both approaches are negatively affected by the number of active MU and synchronization levels. However, STICA provides a more robust MU territory estimation, outperforming STA in all the tested conditions. Our results suggest that spatio-temporal independent component decomposition of TVS is a suitable approach for anatomical and mechanical characterization of single MUs using a combined HDsEMG and ultrafast US approach.

## I. INTRODUCTION

Surface electromyography (sEMG) and ultrasound (US) imaging are used to assess electrical and structural muscle properties respectively. Both techniques underwent significant advancements in the last two decades, providing researchers and clinicians with new tools to investigate the neural and mechanical determinants of muscle force production. The detection and processing of sEMG signals from multiple muscle locations (high-density surface Electromyography; HDsEMG) enabled to describe muscle active contribution to motor tasks both at global level and at single motor unit (MU) level, through decomposition algorithms [1], [2]. The high spatial resolution of B-mode US

image sequences, classically used to extract structural and anatomical muscle properties [3], has been recently complemented with high temporal resolution (frame rates up to few kfps) [4], opening new perspectives on the investigation of mechanical events taking place within short time scales (tens of ms) in the muscle. In this regard, reports in literature showed that the analysis of cross-sectional tissue velocity sequences extracted from ultrafast US [5] allows to access anatomical and mechanical characteristics of single MUs [6]. The progress in both fields suggests that the integration of HDsEMG and high frame rate US has the capability to provide a complete description of the electrical and physical (mechanical and anatomical) MU properties. Moreover, since the two techniques measure different aspects of the same physiological phenomenon, their combination has the potential to improve the current algorithms based on both techniques individually [7]. Here we propose an integrated HDsEMG - Ultrafast US approach to identify anatomical characteristics of single MUs. Briefly, the method extracts single MU firings from HDsEMG [2] and the use of this information to identify the corresponding muscle movements (hereafter referred to as *MU twitching areas*) in US images. The specific aim of this study is to compare two possible methods to perform this integration. The first one is the Spike Triggered Averaging (STA) of the tissue velocity sequence based on the occurrences of individual MU firings, as previously proposed for single MU analysis of mechanomyograms [8]. The second one is based on the Spatio-Temporal Independent Components Analysis (STICA) of the tissue velocity sequences, recently suggested for the processing of ultrafast US muscle images [6]. The comparison of these two approaches was performed in a simulated environment in order to control the conditions leading to the generation of the MU firing patterns and tissue velocity sequences. Specifically, we compared the performance of the two methods in a simulated fusiform muscle by modulating two relevant parameters of muscle contraction: the degree of neural excitation (i.e. number of active MUs) and the level of MU synchronization (i.e. degree of dependency between firing instants of different MUs). The results of this study are expected to provide quantitative evidence on the suitability of the two proposed approaches for anatomical and mechanical characterization single MUs.

M. C., S.Z. and A. B. are with the Laboratory for Engineering of the Neuromuscular System (LISiN), Dipartimento di Elettronica e Telecomunicazioni, Politecnico di Torino and with the Polito<sup>BIO</sup>Med Lab, Politecnico di Torino, Torino, Corso Duca degli Abruzzi 29, 10129 Italy (phone: +39 011-090-7762; e-mail: [alberto.botter@polito.it](mailto:alberto.botter@polito.it)).

K.M.M. and S.S. are with the Biolab, Dipartimento di Elettronica e Telecomunicazioni, Politecnico di Torino and with the Polito<sup>BIO</sup>Med Lab, Politecnico di Torino, Torino.

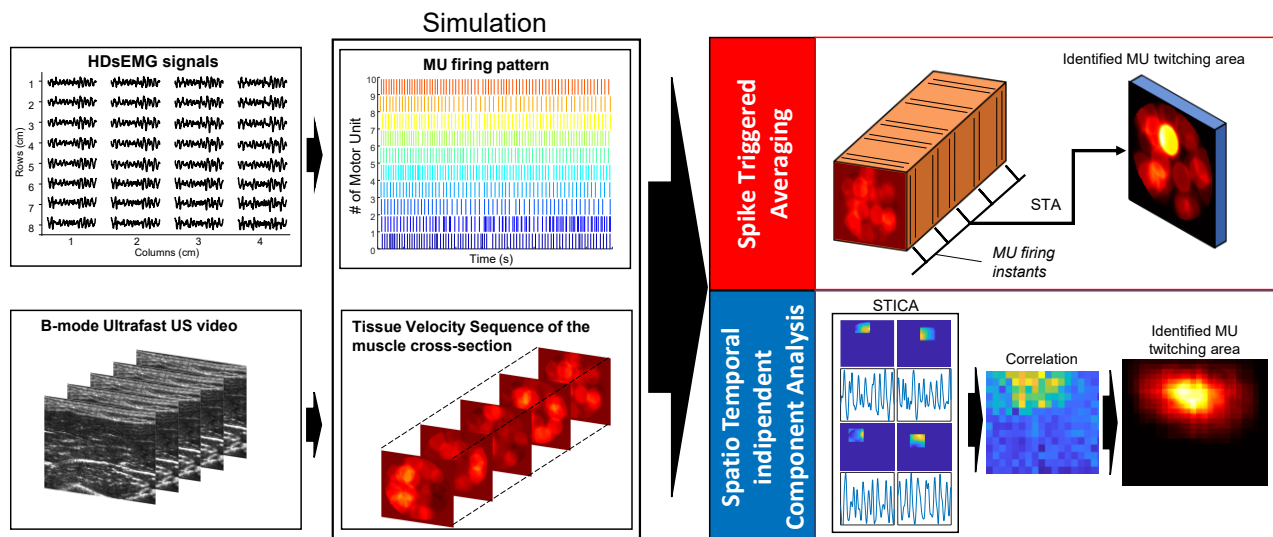


Figure 1. Method for the detection of MU twitching territories through the integration of HDsEMG and ultrafast US. The method combines firing pattern of active MUs (decomposed from HDsEMG) and the analysis of the cross-sectional tissue velocity sequences (estimated from ultrafast US sequences) to identify single MU displacement areas (MU twitching territories) in the muscle cross sections. Two approaches can be adopted to implement this integration. The first one is based on spike triggered averaging (STA, red box) and the second one on spatio-temporal independent component analysis (STICA, blu box).

## II. METHODS

The block diagram of the proposed approach is shown in Figure 1. The method combines the firing pattern of active MUs (decomposed from HDsEMG) and the tissue velocity sequence (obtained from ultrafast US imaging) to identify the MU twitching areas in the muscle cross section. Two algorithms based on spike triggered averaging (STA) and spatio-temporal Independent Components Analysis (STICA) were implemented and tested on simulated data (section B).

### 1) Spike-Triggered Averaging (STA) approach

For each MU we averaged 125-ms epochs of the tissue velocity sequence following every firing instant [8]. We therefore obtained an averaged velocity sequence in which the contribution of the considered MU was emphasized over the others. After removing the mean value from this averaged sequence, we identified the frame at which the maximum velocity occurred. The velocity sequence was averaged across the 20 frames around the maximum (10 frames before and 10 frames after) time sample to obtain a single image. A global thresholding (70% of the maximum) was applied to this image to segment the MU twitching area.

### 2) Spatiotemporal independent component analysis (STICA) approach

We applied STICA to the tissue velocity sequences by extracting regions of interest (ROI) from the image sequences [6]. Singular value decomposition was applied to every ROI retaining the 50 most significant components and finally optimizing spatio-temporal independence between components through independent component analysis over space and time. Afterwards, for each MU we computed the convolution between its firing instants and a synthetic waveform representing the velocity of contracting fibers in the superficial-deep axis [4]. This convolution produced what we refer to as the *train of MU velocity twitches*. We computed the cross-correlation between these trains and each of the temporal independent components obtained for each ROI. For each ROI we selected the component with the maximum correlation

within a  $\pm 20$  ms time lag. This procedure provided a map of correlation coefficients for each decomposed MU, in which each pixel represented a ROI and its color is scaled with the peak of the cross-correlation. We segmented the correlation map to retain ROIs with correlation values higher than 50% and then identified the largest group (cluster) of connected ROIs providing the greatest mean correlation value. The spatial components of the ROIs corresponding to the identified cluster were summed to obtain the spatial representation of single MUs in the image. Similarly to the STA approach, a global thresholding 70% of the maximum) was applied to this image to determine the MU twitching area.

### B. Simulation Model

The performance of the two approaches described in the previous section were assessed in simulated conditions. We simulated the MU firing patterns and the tissue velocity sequences of a muscle contracting at four contraction levels with two degrees of MU synchronization. The simulations were based on a cylindrical volume conductor model with skin-parallel fibers [9]. The simulated muscle had an elliptical, physiological cross-sectional area of 598 mm<sup>2</sup> (Fig. 2a) and 80,000 muscle fibers uniformly distributed in the muscle cross-section (i.e. fiber density of about 135 fib/mm<sup>2</sup>). A population of 200 MUs (Fig. 2a) with circular territory randomly distributed throughout the muscle (number of MU fibers ranged from 150 to 1500) was simulated.

#### 1) MU firing patterns

A model of recruitment of MUs [10] was applied to simulate the firing patterns of active MUs during four 10-s steady contractions at constant percentage of maximum voluntary contraction (MVC). We simulated a total number of 32, 74, 106 and 138 active MUs for 2%, 5%, 10% and 20% MVC respectively. For each contraction we implemented 2 degrees of synchronization between active MUs by modifying the firing patterns with the procedure proposed by Yao et al [11]. A medium level (15%) and a very high level (25%) [12] of MU synchronization were considered.

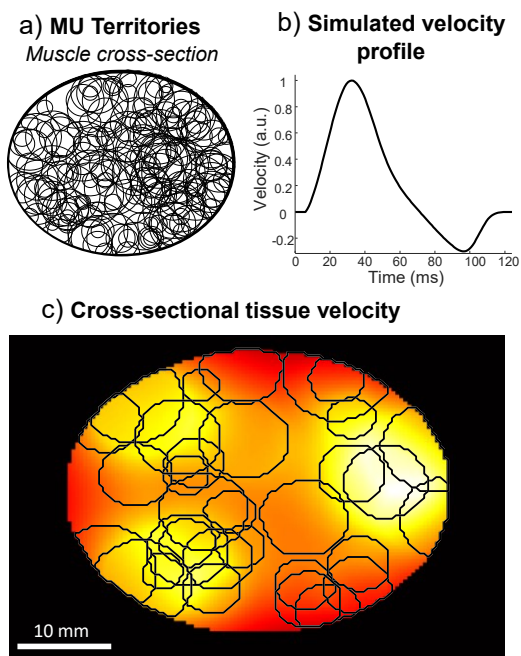


Figure 2. a) Distribution of MU territories (area range 5 - 44 mm<sup>2</sup>) in the muscle cross-section. b) Normalized velocity profile of the tissue velocity simulation model [6]. c) example of a frame of the simulated TVS at 2% MVC with the location of the 32 active MUs (gray circles).

## 2) Tissue velocity sequences

Tissue velocity sequences (TVS) were simulated at 1024 fps. The size of the images was 128 × 128 pixels, corresponding to a spatial resolution of 0.3 mm for a field of view of 40 mm × 40 mm (Fig. 2c). The interferential tissue velocity sequence of the simulated contractions was obtained by combining the MU firing patterns and a model of mechanical responses of single MUs. This model describes the spatiotemporal velocity profiles of the MU fibers in the muscle cross-section in response to a single firing. Briefly, for each MU we considered the normalized velocity twitch representing the contraction (positive) and relaxation (negative) phases of a group of excited fibers (Fig. 2b) [4]. We associated this velocity twitch to each pixel of the tissue velocity sequence included in the MU territory and we scaled its amplitude with the area of the territory using a quadratic law [4]. To simulate the passive transmission of velocity to the surrounding non-active fibers, we used a bidimensional exponential decay centered on the MU territory to scale the amplitude of the velocity twitches of the pixels outside the MU territory. The decay rate varied between MU and was defined so that the tissue velocity at a distance of twice the MU territory radius was 50% of the velocity at the center of the territory.

## C. Performance Evaluation

The comparison between the MU twitching territories computed with STA and STICA and the simulated ones was based on geometrical variables (errors of center and area estimations). Specifically, we considered: (i) the Euclidean distance between the center of the simulated and the computed territories and (ii) the absolute difference between the area of computed and simulated MU territories, divided by the size of the simulated one. Finally, we calculated the relative number of MU territories correctly identified w.r.t. to the total number

of simulated MUs. A MU territory was regarded as correctly identified if the variables *Recall* and the *Precision* [13] were both greater than 0.4.

## D. Statistical analysis

The errors of centers/areas estimations were merged into two datasets according to the method (STA or STICA) and analyzed with one-way ANOVA (factor: “method”). The effect of the factors “force level” and “synchronization level” were tested with a 2-way ANOVA separately on the method and type of error. Post-hoc assessments were conducted using Bonferroni test whenever a main effect was verified. Significance was set at  $p < 0.05$ .

## III. RESULTS AND DISCUSSION

Figure 3a shows the comparison between a representative, simulated MU territory and the correspondent estimates in two different conditions. The left image refers to a 2% MVC contraction with 15% Synchronization (good identification of MU territory; Precision = 0.78 and Recall = 0.79), while the right one to a 20% MVC contraction with 25% Synchronization (poor identification of MU territory; Precision = 0.12 and Recall = 0.35). Based on the criteria described in section C, the left MU was correctly identified, while the right one was regarded as a wrong identification.

Group analyses confirmed the single case observation depicted in Figure 3a. Indeed, both the contraction level and the degree of synchronization degraded the performance of MU territory identification in terms of territory estimation errors (Figure 3c) and consequently also the percentages of correct identification (Figure 3b). This result was due to the larger number of sources (MUs) activated for higher contraction levels (see B1) and to the reduced independency between their activation instants, associated with the higher degree of synchronization. Both these aspects are well known factors compromising the capability of STA and STICA to isolate the constituting contributions of the global signal and suggest a limited applicability of these methods for high contraction levels.

The comparison between the two methods showed that STICA was able to correctly identify a larger number of MU territories than STA (Figure 3b). A significant effect of the contraction level and degree of MU synchronization was observed for both methods. However, the percentage of correct MU identification decreased to a lower extent for STICA (78% to 34%) than for STA (37% to 1%) between 2% and 20% MVC. Similar results were observed for the comparison at different levels of MU synchronization. While the percentage of correct identification decreased of 3% (at 2%MVC) and 13% (at 20% MVC) for STICA, STA failed (i.e. 0% of MU detected) for 10% and 20% MVC.

Boxplots in Figure 3c show the errors on centers (top panels) and areas (bottom panels) of the MU territory estimates obtained with STICA (blue) and STA (red), for the considered contraction and synchronization levels. STICA approach provided lower errors in identifying both MU territories centers and areas for all tested conditions, as demonstrated by a statistically significant differences with respect to the STA approach ( $p < 0,05$ ). Center and area errors increased with contraction and synchronization levels to a greater extent for STA than for STICA. This evidence, together with the



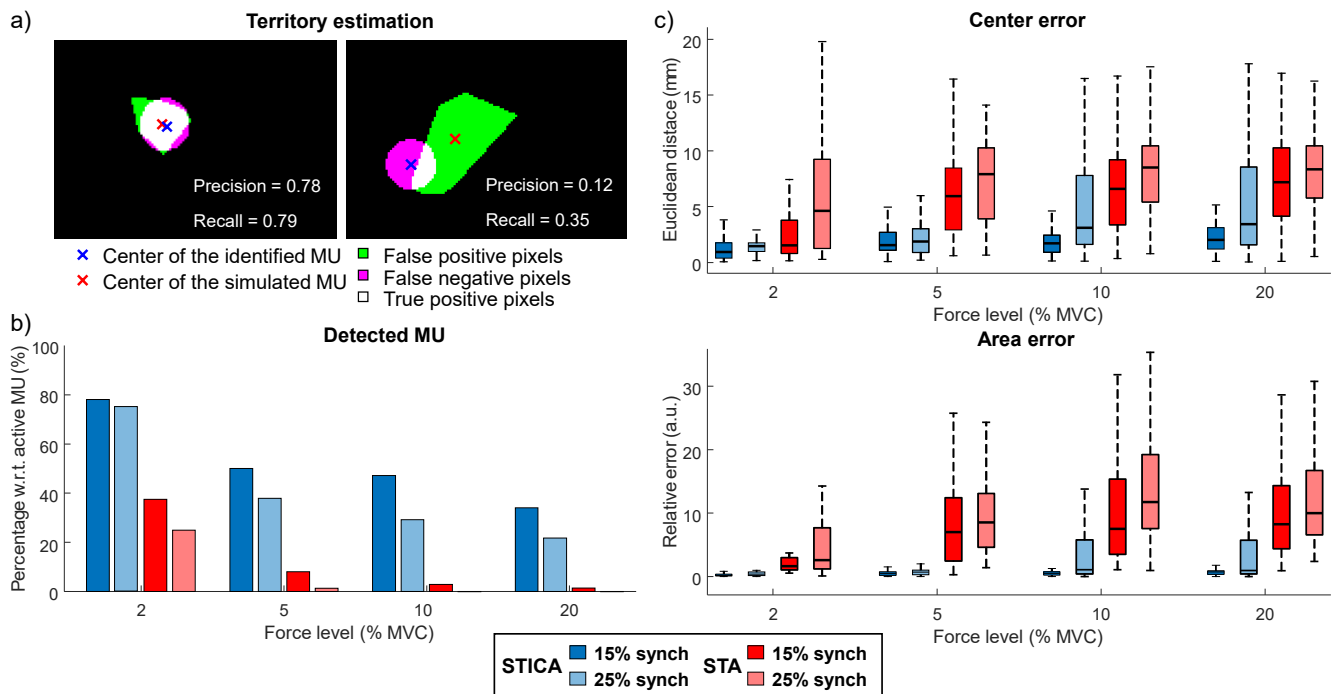


Figure 3. a) Two examples of MU territory estimates (white and green pixels) superimposed to the simulated ones (white and pink pixels). White areas include the correctly identified pixels (true positive), while pink and green areas denote the false negative and false positive pixels respectively. The crosses indicate the center of identified (red) and simulated (blue) MU territory. b) Percentage of the correctly identified MU territories w.r.t. the number of active MUs for the two methods (STICA and STA) applied to simulated contractions at different contraction and MU synchronization levels. c) Boxplots of center and area errors for methods, contractions and synchronization levels.

percentage of correct identification, suggests that STICA is less affected by the increasing number of active MUs than STA.

Overall, our results showed that STICA provides a more robust MU territory estimation than STA, likely because it exploits both spatial and temporal information of the sources. It is important to note that since the two approaches rely on the linear summation of the individual MU contributions, possible non linearities affecting experimental signals may degrade the described performance.

#### IV. CONCLUSIONS

In this study we compared two approaches (STA and STICA) to identify MU twitch territories from the tissue velocity sequences detected in muscle cross-sectional images. We showed that STICA outperformed STA in identifying the location of MU territories at different contraction and synchronization levels. Our results provide quantitative evidence on the suitability of the two proposed approaches for anatomical mechanical characterization of single MUs using a combined HDsEMG and ultrafast US approach.

#### REFERENCES

- [1] R. Merletti, M. Avettaggiato, A. Botter, A. Holobar, H. Marateb, and T. M. M. Vieira, "Advances in surface EMG: Recent progress in detection and processing techniques," *Crit. Rev. Biomed. Eng.*, vol. 38, no. 4, pp. 305–45, 2010, doi: 10.1615/CritRevBiomedEng.v38.i4.10.
- [2] A. Holobar and D. Zazula, "Correlation-based decomposition of surface electromyograms at low contraction forces," *Med. Biol. Eng. Comput.*, vol. 42, no. 4, 2004, doi: 10.1007/BF02350989.
- [3] P. W. Hodges, L. H. M. Pengel, R. D. Herbert, and S. C. Gandevia, "Measurement of muscle contraction with ultrasound imaging," *Muscle and Nerve*, vol. 27, no. 6, pp. 682–692, 2003, doi: 10.1002/mus.10375.
- [4] T. Deffieux, J. L. Gennisson, M. Tanter, and M. Fink, "Assessment of

- the mechanical properties of the musculoskeletal system using 2-D and 3-D very high frame rate ultrasound," *IEEE Trans. Ultrason. Ferroelectr. Freq. Control*, vol. 55, no. 10, pp. 2177–2190, 2008, doi: 10.1109/TUFFC.917.
- [5] T. Loupas, R. W. Gill, and J. T. Powers, "An Axial Velocity Estimator for Ultrasound Blood Flow Imaging, Based on a Full Evaluation of the Doppler Equation by Means of a Two-Dimensional Autocorrelation Approach," *IEEE Trans. Ultrason. Ferroelectr. Freq. Control*, vol. 42, no. 4, pp. 672–688, 1995, doi: 10.1109/58.393110.
- [6] R. Rohlfen, E. Stålberg, and C. Grönlund, "Identification of single motor units in skeletal muscle under low force isometric voluntary contractions using ultrafast ultrasound," *Sci. Rep.*, vol. 10, no. 1, pp. 1–11, 2020, doi: 10.1038/s41598-020-79863-1.
- [7] A. Botter, T. M. Vieira, I. D. Lorum, R. Merletti, and E. F. Hodson-Tole, "A novel system of electrodes transparent to ultrasound for simultaneous detection of myoelectric activity and B-mode ultrasound images of skeletal muscles," *J. Appl. Physiol.*, vol. 115, no. 8, pp. 1203–1214, 2013, doi: 10.1152/jappphysiol.00090.2013.
- [8] C. Cescon, M. Gazzoni, M. Gobbo, C. Orizio, and D. Farina, "Non-invasive assessment of single motor unit mechanomyographic response and twitch force by spike-triggered averaging," *Med. Biol. Eng. Comput.*, vol. 42, no. 4, pp. 496–501, 2004, doi: 10.1007/BF02350990.
- [9] D. Farina, L. Mesin, S. Martina, and R. Merletti, "A Surface EMG Generation Model with Multilayer Cylindrical Description of the Volume Conductor," *IEEE Trans. Biomed. Eng.*, vol. 51, no. 3, 2004, doi: 10.1109/TBME.2003.820998.
- [10] A. J. Fuglevand, D. A. Winter, and A. E. Patla, "Models of recruitment and rate coding organization in motor-unit pools," *J. Neurophysiol.*, vol. 70, no. 6, pp. 2470–2488, 1993, doi: 10.1152/jn.1993.70.6.2470.
- [11] W. Yao, A. J. Fuglevand, and R. M. Enoka, "Motor-unit synchronization increases EMG amplitude and decreases force steadiness of simulated contractions," *J. Neurophysiol.*, vol. 83, no. 1, pp. 441–452, 2000, doi: 10.1152/jn.2000.83.1.441.
- [12] D. Farina, L. Fattorini, F. Felici, and G. Filligoi, "Nonlinear surface EMG analysis to detect changes of motor unit conduction velocity and synchronization," *J. Appl. Physiol.*, vol. 93, no. 5, pp. 1753–1763, 2002, doi: 10.1152/jappphysiol.00314.2002.
- [13] A. A. Taha and A. Hanbury, "Metrics for evaluating 3D medical image segmentation: Analysis, selection, and tool," *BMC Med. Imaging*, vol. 15, no. 1, 2015, doi: 10.1186/s12880-015-0068-x.